PHYSICAL REVIEW RESEARCH **7**, L042003 (2025)

Letter

# Quantum Zeno blockade in optomechanical systems

Karl Pelka * and André Xuereb †

*Department of Physics, University of Malta, Msida MSD 2080, Malta*

(Received 24 January 2025; revised 28 August 2025; accepted 9 September 2025; published 2 October 2025)

We investigate the application of the quantum Zeno effect (QZE) for the preparation of non-Gaussian states in optomechanical systems. By frequently monitoring the system, the QZE can suppress transitions away from desired subspaces of states. We show that this enables the preparation of states in qubit subspaces even in the presence of noise and decoherence. Through analytical and numerical analysis, we demonstrate that QZE-based protocols can achieve robust state preparation of qubit states in continuous variable architectures. Our results extend the utility of the QZE beyond discrete systems, highlighting its potential for enhancing quantum control in more complex quantum information processing environments. These findings offer a promising approach for achieving reliable non-Gaussian states in optomechanical systems, with implications for the development of photonic quantum computing and quantum sensing.

DOI: 10.1103/vhnq-79bj

*Introduction.* Originally conceived as a Gedanken experiment showcasing the absurdity of frequent measurements in quantum mechanics [1], the quantum Zeno effect has shown in a multitude of systems to suppress the decay of unstable quantum systems [2–6], stop coherent dynamics [7,8], or tunneling processes [9]. Another consequence is that the effect can inhibit the evolution of the system away from a desired Hilbert subspace, effectively "freezing" it in a particular set of states, which allows the dynamical manipulation of the quantum system by frequently [10,11] or continuously [12] monitoring a quantum system [13]. This aspect can be leveraged as a means of controling quantum transitions and manipulate quantum states with high precision for cavity QED systems [8,14,15] and hybrid cavity-qubit systems [12]. Among the various techniques available, the quantum Zeno effect has emerged as a powerful tool for robust state preparation in noisy environments, which is fundamental to the realization of quantum technologies.

Under the auspices of cavity optomechanics [16], recent theoretical and experimental advances have demonstrated the potential carried by systems experiencing radiation pressure for fundamental investigations as well as technological applications [17]. The radiation in a single mode of the electromagnetic radiation field, e.g., within an optical cavity with a high finesse driven by a pump field from an external waveguide [18], experiences a dispersive shift and exerts a force on the motion of a harmonic oscillator through the radiation pressure force to comprise the prototypical optomechanical system [19]. The mechanical element comes in many guises such as a micro- or nanoparticle in the cavity [20,21], a semitransparent membrane inside the cavity [22], one of the end mirrors of the cavity [23], one plate of a capacitor [24], or the cavity itself in the case of microtoroids supporting whispering gallery modes of the radiation field [18]. Mediated through dielectric forces, those mechanical systems can be driven directly and parametrically in superconducting cavities [25,26] and other nanoelectromechanical setups [27]. The combination of quantum-noise-limited optical control with high mechanical coherence allows for quantum transducers [28,29], directional amplifiers for microwave radiation [30–33], and enables mechanical frequency combs [34]. Optomechanical interactions can be exploited to create entanglement between macroscopic mechanical oscillators [35–38], cool mechanical systems to their quantum ground state [24,39], and create parametric oscillations [40]. Multimode systems can exploit these self-sustained oscillations for synchronization phenomena [41–45] and can display distinct behavior based on temporal driving schemes [46–49] or many-body dynamics in complex networks [50–53]. Radiation pressure can also be used to realize a variety of interactions between the constituents beyond linear dispersive shifts, such as quadratic ones [22,54–57] or cross-Kerr couplings [58,59].

In this Letter, we study the restriction of bosonic systems to a subset of possible states through nonlinearities. We demonstrate that this effectively achieves a photon blockade distinct from the known one in the strong optomechanical coupling regime [60] as well as a novel phonon blockade. We show that the blockade constrains the system's Hilbert space to qudits of arbitrary dimension and that the required parameter regime can be achieved in state-of-the-art experiments. Moreover, this proposed scheme allows the generation of mechanical Fock states with high fidelity with simple drive tones avoiding quantum control schemes on the drive [61,62]. Our findings provide a technique for potential applications of

*Contact author: karl.a.pelka@um.edu.mt
†Contact author: andre.xuereb@um.edu.mt

optomechanical systems as quantum nonlinear devices, with significant relevance for optical quantum computation, photonic quantum simulation schemes, or quantum information processing [63].

We proceed by discussing the minimal setup to generate the quantum Zeno effect in closed bosonic systems through strong continuous couplings [64]. This analysis will allow us to gain the intuition for the occurring physics. We will then show that the effect carries over to achievable optomechanical coupling schemes that will introduce the effective phonon blockade. Through numerical analysis of quantum optical master equations, we assess the impact of environmental noise and decoherence and confirm that the blockade can be tested in state-of-the-art experiments in spite of thermalization with an environment and far from the optomechanical strong coupling regime. Ultimately, we conclude with a discussion on the implication of our results.

*Effective model.* We consider the dynamics of two driven bosonic modes that are described by the Hamiltonian

$$\frac{\hat{H}}{\hbar} = \omega \hat{a}^\dagger \hat{a} + \Omega \hat{b}^\dagger \hat{b} + g\hat{O} + [iEe^{i\omega_L t}\hat{a} + iDe^{i\Omega_D t}\hat{b} + \text{H.c.}], \tag{1}$$

with $\hat{a}$ ($\hat{b}$) describing the bosonic annihilation operators of the optical (mechanical) mode, $\omega$ ($\Omega$) their respective resonance frequencies, $g$ the strength of the coupling described by the operator $\hat{O}$. The parameters $|E| = \sqrt{2\mathcal{P}_L\kappa/\hbar\omega_L}$ ($|D| = \sqrt{2\mathcal{P}_D\gamma/\hbar\Omega_D}$) describe the strength of the optical (mechanical) drive occurring at $\omega_L$ ($\Omega_D$) in relation to the drive's input power $\mathcal{P}_L$ ($\mathcal{P}_D$) and mode's decay rate $\kappa$ ($\gamma$). We proceed to analyze our system using the strong continuous coupling mechanism that leads to the quantum Zeno effect [64]. This formulation assumes a Hamiltonian being the sum of a measurement Hamiltonian $K\hat{H}_c$ modeling the continuous measurement, and a remainder $\hat{H}_o(t)$ describing the system under observation. In the limit of a strong coupling constant $K$, the evolution operator $\hat{\mathcal{U}}_K(t)$ approaches the operator $\lim_{K\to\infty}\hat{\mathcal{U}}_K(t) = \mathcal{T}\exp(-\frac{i}{\hbar}\int_0^t \hat{H}_Z(\tau)\mathrm{d}\tau)$ with the Zeno Hamiltonian

$$\hat{H}_Z(t) = K\hat{H}_c + \sum_j \hat{P}_j \hat{H}_o(t)\hat{P}_j, \tag{2}$$

where $\hat{P}_j$ denotes the projection operators onto the eigenspaces of $\hat{H}_c$ with the respective eigenvalue $\eta_j$. Since this projection turns the Hamiltonian of the observed system into block diagonal form, there can be no transition between the distinct eigenspaces $\mathcal{H}_{\hat{P}_j}$ and the quantum Zeno effect occurs.

We counterintuitively identify the system under observation with the drive $\hat{H}_o(t) = [i\hbar Ee^{i\omega_L t}\hat{a} + i\hbar De^{i\Omega_D t}\hat{b} + \text{H.c.}]$ and the measurement Hamiltonian with the bosonic modes and their interaction $\hat{H}_c = \hbar\omega\hat{a}^\dagger\hat{a} + \hbar\Omega\hat{b}^\dagger\hat{b} + \hbar g\hat{O}$ to conduct the analysis of the system described by Eq. (1). We begin the investigation with a cross-Kerr interaction described by $\hat{O} = \hat{a}^\dagger\hat{a}\hat{b}^\dagger\hat{b}$ as displayed in Fig. 1. In this case, number states $|n\rangle \otimes |m\rangle$ remain eigenstates of $\hat{H}_c$ and the energy spectrum is $E_{nm} = \hbar(\omega n + \Omega m + gmn)$ as displayed in Fig. 1(b). This interaction allows us to go into the rotating frame (see Supplemental Material [65]) and rewrite the Zeno Hamiltonian in

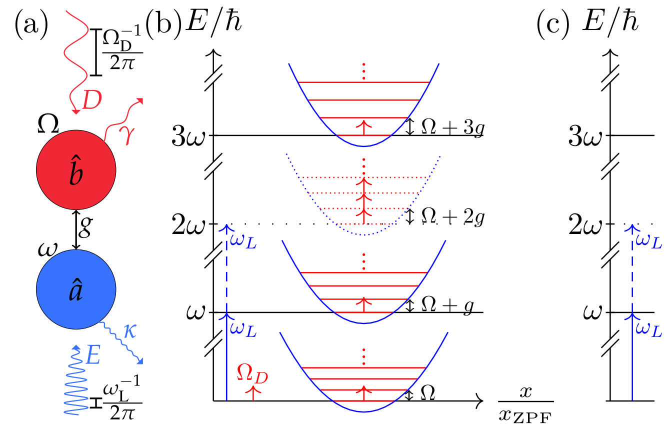


FIG. 1. Quantum Zeno effect in an optomechanical cavity. (a) An optomechanical system consisting of a mechanical and an optical mode, both driven at distinct frequencies coupled nonlinearly. (b) A cross-Kerr nonlinearity enables a mechanical drive to address mechanical transitions solely for a particular photon number. The resonant states of the mechanical drive form a Zeno subspace, which makes them inaccessible from the rest of the states. (c) The photonic spectrum lacks the state with the photon number tunable via the mechanical drive frequency, and hence, a photon blockade occurs.

Eq. (2) in a suggestive manner,

$$\hat{H}_B/\hbar = \Delta\hat{a}^\dagger\hat{a} + (\delta + g\hat{a}^\dagger\hat{a})\hat{b}^\dagger\hat{b} + \sum_k \hat{P}_k\hat{H}_o\hat{P}_k, \tag{3}$$

with the optical (mechanical) detuning $\Delta = \omega - \omega_L$ ($\delta = \Omega - \Omega_D$). The strong coupling limit requires in this case that the driving strengths $D$ and $E$ have to be much smaller than the frequencies $\omega$, $\Omega$, and $|g|$.

We can determine the frequency spectrum of this Hamiltonian as $\tilde{\omega}_{nm} = \Delta n + (\Omega - \Omega_D + gn)m$ and see that the frequency of the mechanical drive can be tuned to enable an infinite-dimensional degeneracy: If the drive frequency is tuned to $\Omega_D = \Omega + gN$ with $N \in \mathbb{N}$ we find that all states $|N\rangle \otimes |m\rangle$ are degenerate with the eigenvalue $\eta_N = \Delta N$. The mechanical drive with this particular frequency is resonant with the energy ladder of the mechanical oscillator if and only if $N$ photons are present in the optical mode, as shown in Fig. 1(b) for the case of $N = 2$ photons. In our further analysis, we employ $N = 2$ noting that choosing any other $N$ restricts the Hilbert space of the bosonic system to that of the corresponding qudit, transcending the capabilities of known Zeno blockade schemes [14,15]. Moreover, we find that for any finite optical detuning ($\Delta \neq 0$), the eigenvalue is different from all states with $n \neq N$ as

$$\tilde{\omega}_{nm} = \Delta n + (g(n - N))m. \tag{4}$$

This means that a mechanical drive tuned to the frequency $\Omega_D = \Omega + gN$ enables the removal of the state with $N$ excitations from the optical mode for an arbitrary $N \in \mathbb{N}$, making it inaccessible from the remaining states. Thus, the quantum Zeno effect from strong continuous coupling [64] permits to dynamically constrain a fully bosonic system into a discrete qudit system as illustrated for $N = 2$ in Fig. 1(c). The quintessential feature that allows the blockade is the introduction of a frequency shift $\omega_Z(n, m)$ through the interaction in

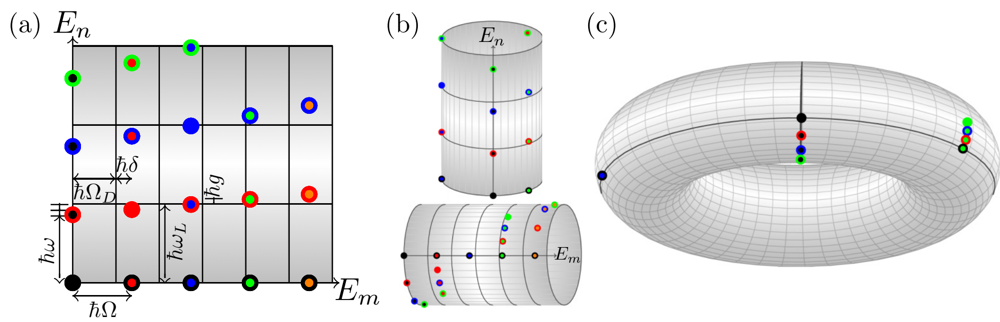


FIG. 2. Emergence of quantum Zeno dynamics through cross-Kerr interaction. (a) A two-dimensional arrangement of energy eigenvalues shows that the energy spacing for the addition of a photon grows with the phonon number. (b) The invariant Zeno subspaces are found by coalescence of the energy eigenvalues when rolling up the energy plane with the periodicity given by the drive frequencies. (c) We see that the laser drive allows to select the invariant subspace, here all states with two phonons indicated by a blue interior, which are inaccessible from the remaining levels.

the spectrum $\tilde{\omega}_{nm} = (\omega - \omega_L) + (\omega - \omega_D) + \omega_Z(n, m)$. This allows to uniquely select the transitions that are desired to be suppressed by tuning the drive $\Omega_D = \Omega + \omega_Z(N, m)$ for a photon blockade of level $N$. Additionally, we prove that this result persists with arbitrary perturbing interactions and numerically demonstrate it specifically for dispersive optomechanical coupling of the form $\hbar g_0 \hat{a}^\dagger \hat{a}(\hat{b}^\dagger + \hat{b})$ (see Supplemental Material [65]).

To give this result a more physical interpretation, we evaluate the Hamiltonian in this removed subspace, described by the projector $\hat{P}_{Nm} = |N\rangle\langle N| \otimes \mathbb{1}_B$. We find in this case that $\hat{H}_N/\hbar = \Delta \hat{a}^\dagger \hat{a} + iD(\hat{b}^\dagger - \hat{b})$ and see that the mechanical system would be driven if the optical state acquired the removed amount of excitations. Thus, the mechanism behind this quantum Zeno effect is revealed to lie in the resonance of the mechanical drive: If the optical system were to achieve the amount of excitations such that the mechanical drive becomes resonant with the mechanical mode, the drive would transmit energy into the mechanical mode. Since this transmission of energy is only possible on resonance, it would enable to draw conclusions about the optical state constituting a measurement.

It is worth noticing that the cross-Kerr interaction maintains the symmetry of the measurement Hamiltonian under exchange of the operators $\hat{a} \leftrightarrow \hat{b}$, and therefore the optical drive likewise enables the tunable removal of the state with $M$ excitations from the mechanical mode for $\omega_L = \omega + gM$ or more generally $\omega_L = \omega + \omega_Z(n, M)$. The structure of the distinct Zeno subspaces can be determined geometrically (see Supplemental Material [65]) and is displayed for this case in Fig. 2. The energy eigenvalues $E_{nm}$ are arranged on a two-dimensional plane in Fig. 2(a) such that the sum of the Cartesian coordinates add up to the respective value. Here, the color of the inner circle describes the optical quantum number $n$ and the outer ring has the same color for all states with the same mechanical quantum number $m$. Figure 2(b) illustrates the plane wrapped up with the periodicities given by the drive frequency $\Omega_D$ in the upper diagram and with $\omega_L = \omega + 2g$ in the lower diagram. Note that in the upper case all points are scattered around the cylinder while in the lower case all points representing eigenvalues with the mechanical quantum number $M = 2$, indicated by a blue interior, coalesce. Wrapping up each cylinder around the remaining axis results in the torus shown in Fig. 2(c). The invariant Zeno subspaces can be determined by the coalescence of the respective eigenvalues, in this case *span*$(|n\rangle \otimes |2\rangle)$, and those states become inaccessible from the remaining states in the strong coupling limit.

*Optomechanical realization.* To confirm that the quantum Zeno effect remains with finite coupling strengths and decay into a thermal environment, we conduct numerical simulations of the corresponding quantum optical master equation. The optical (mechanical) mode decays with the rate $\kappa$ ($\gamma$) into its bath at temperature $T$, realized with the standard dissipator in Lindblad form $\mathcal{D}_{\hat{o}}[\rho] = \hat{o}\rho\hat{o}^\dagger - \frac{1}{2}\{\rho, \hat{o}^\dagger\hat{o}\}$. The dynamics of the system's density matrix $\rho$ are described by the master equation in Lindblad form [66],

$$\dot{\rho} = -\frac{i}{\hbar}[\hat{H}, \rho] + \kappa\{(\bar{N} + 1)\mathcal{D}_{\hat{a}}[\rho] + \bar{N}\mathcal{D}_{\hat{a}^\dagger}[\rho]\} + \gamma\{(\bar{M} + 1)\mathcal{D}_{\hat{b}}[\rho] + \bar{M}\mathcal{D}_{\hat{b}^\dagger}[\rho]\}, \quad (5)$$

where the temperature $T$ determines the average occupation $\bar{N} = [\exp(\hbar\omega/k_B T) - 1]^{-1}$ ($\bar{M} = [\exp(\hbar\Omega/k_B T) - 1]^{-1}$) of the optical (mechanical) mode. Throughout the simulations, we employ parameters adapted from Refs. [58,59,67] and the quantum ground state $\rho_0 = |0\rangle\langle 0| \otimes |0\rangle\langle 0|$ is used as the initial state. Concretely, we consider a cavity with an optical frequency of $\omega/2\pi = 5$ GHz and decay rate $\kappa/2\pi = 64.8$ kHz and a mechanical mode with the frequency $\Omega/2\pi = 65$ MHz and decay rate $\gamma/2\pi = 10$ kHz coupled with the coupling strength of $g/2\pi = -2.7$ MHz to each other. Both modes are in contact with environments thermalized at $T = 20$ mK, which amounts to $\bar{M} = 0.267$ and $\bar{N} = 6.46 \times 10^{-6}$. Further nonlinearities that could occur were investigated, and their impact on the scheme is negligible (see Supplemental Material [65]). Figure 3 summarizes the characteristics of the resulting state of the mechanical oscillator $\rho_B(t) = \mathrm{Tr}_A \rho(t)$ for the mechanical drive $D^{(1)}/|g| = 0.02$ at the frequency $\Omega_D = \Omega$ for optical drives of varying strength $E^{(0)}/|g| = 0$ (dashed), $E^{(1)}/|g| = 0.25$ (dotted), and $E^{(2)}/|g| = 0.75$ (solid) at the frequency of the second photon level $\omega_L = \omega + 2g$. Figure 3(a) shows the occupation probabilities of the mechanical ground state $P_0$ (black), the mechanical state containing one phonon $P_1$ (red), and the second excited mechanical state $P_2$ (blue). For absent optical drive (dashed), the mechanical drive excites phonons, leading to an increase in

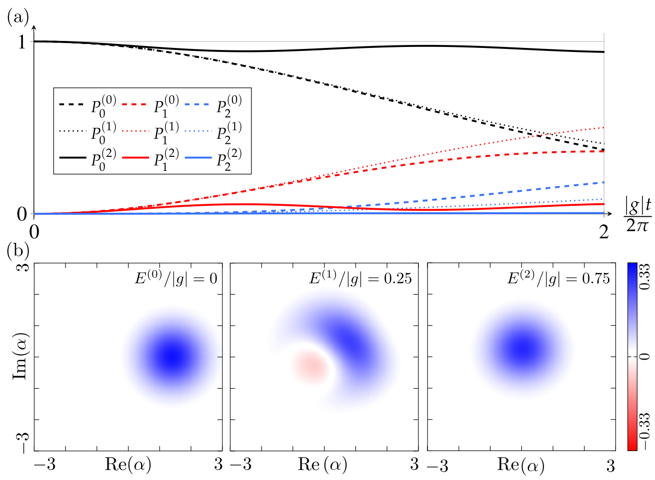


FIG. 3. Analysis of resulting state from the quantum Zeno dynamics for the open system driven with $D^{(2)}/|g| = 0.065$ at frequency $\Omega_D = \Omega$. (a) Probability to find zero (black), one (red), and two (blue) phonons in the mechanical subsystem over time for optical drive with $E^{(0)}/|g| = 0$ (dashed), $E^{(1)}/|g| = 0.25$ (dotted), and $E^{(2)}/|g| = 0.75$ (solid) at frequency $\omega_L = \omega + 2g$. (b) Resulting Wigner function for $E^{(0)}/|g| = 0$ in the left panel showing a displacement of the mechanical state, $E^{(1)}/|g| = 0.25$ in the middle panel showing the occurrence of negative patches indicating the non-Gaussian state, and $E^{(2)}/|g| = 0.75$ disabling the displacement of the mechanical state.

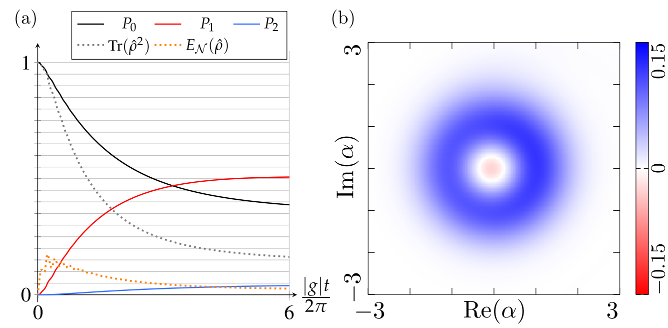


FIG. 4. Analysis of the resulting state from the quantum Zeno dynamics for the open system driven with $E^{(2)}/|g| = 0.75$ at frequency $\omega_L = \omega + g$ and with $D^{(2)}/|g| = 0.065$ at frequency $\Omega_D = \Omega$. (a) Probability to find zero (black), one (red), and two (blue) phonons in the mechanical subsystem over time, showing a strong suppression of two or more phonons. Characterization of the quantum state through purity (gray, dashed) and logarithmic negativity (orange, dashed). (b) Resulting Wigner function of the final state displaying a clear negative patch signaling the non-Gaussian nature of the state in the mechanical subsystem.

the probability of one and two phonons, while the probability to remain in the ground state deteriorates. The left panel of Fig. 3(b) shows the corresponding Wigner function and that without an optical drive establishing a phonon blockade the final state of the mechanical subsystem is a displaced state. Establishing the blocking tone at the intermediate drive amplitude $E^{(1)}$ (dotted lines), we see the increase to find one or zero phonon in the subsystem, while the state with two phonons is suppressed, and more than two phonons do not occur. This signifies that the phonon blockade due to the quantum Zeno effect through intermediate optical drive at $\omega_L = \omega + Mg$ makes states with more than $M$ phonons effectively inaccessible from the quantum ground state $\rho_0$. The middle panel of Fig. 3(b) shows that the corresponding Wigner function has a negative patch signifying the quantum nature of the state in the mechanical subsystem. Further increasing the optical drive amplitude to $E^{(2)}$ (solid lines) results in a strong suppression of the first excited phonon state and a complete suppression of the second phonon state. The right panel of Fig. 3(b) shows that with the increased power of the blocking tone, the final state has negligible occupation for two phonons or more, which indicates that the quantum Zeno blockade removing the states with two phonons is in full effect. The requirement $E \ll |g|$ for the strong coupling regime ceases to hold when increasing the drive strength $E$ even further, which suggests a breakdown of the blockade.

The observation that the phonon blockade for intermediate couplings effectively suppresses the occupation of more than $M$ phonons in the mechanical subsystem can be used to restrict the mechanical subsystem to the ground state and first excited state, effectively modeling a qubit. Thus, we simulate the system with the optical drive amplitude $E^{(2)}/|g| = 0.75$ at frequency $\omega_L = \omega + g$ and mechanical drive $D^{(2)}/|g| = 0.065$ on resonance ($\Omega_D = \Omega$) while all other parameters remain the same and find the behavior illustrated in Fig. 4. In Fig. 4(a), we see that the driving conditions lead to a state where probability for more than one phonon in the cavity is strongly suppressed. Crucially, the probability for one phonon, which indicates the fidelity of the Fock state $|1\rangle$ with the generated state, is dominant. Moreover, we find the created two-mode state is a mixed state as evidenced by the decay of the purity $\mathrm{Tr}(\hat{\rho}^2(t))$ and approaches a separable state since the logarithmic negativity $E_{\mathcal{N}}(t)$ decays after an initial increase. The resulting Wigner function is shown in Fig. 4(b) and shows a negative patch in the center of phase space, reminiscent of the Wigner function of the Fock state $|1\rangle$. Indeed, we find that a cavity with decreased linewidth $\tilde{\kappa} = 0.1\kappa$ allows the creation of the Fock state $|1\rangle$ with a fidelity of larger than 0.9 while both purity and logarithmic negativity decay much slower by using an optical drive with multiple frequencies and intermediate amplitudes (see Supplemental Material [65]). Our investigations show that the quantum Zeno blockade allows to create genuine mechanical quantum states required in quantum sensing with current state-of-the-art experiments, while rapid advances in experimental designs bear the potential to controllably create mechanical Fock states with high fidelity.

*Conclusion and outlook.* We have demonstrated the quantum Zeno effect in an optomechanical system with the goal of preparing qubit states within a purely bosonic system. Our results suggest that quantum Zeno dynamics provide a viable pathway for precise qubit initialization by leveraging the inherent quantum dynamics even in the presence of environmental noise and decoherence. The findings open up avenues for integrating protocols based on the quantum Zeno effect in state-of-the-art optomechanical systems even despite decoherence in an open environment, enabling them to be used in qubit-based quantum information processing, offering broad potential across various quantum computing platforms. Optomechanical systems with an insufficient anharmonicity due to the standard optomechanical dispersive shift may benefit from the Zeno blockade by enabling a dynamic photon blockade through external drive parameters. Systems realizing quadratic optomechanical coupling [22,54–57] incorporate the required cross-Kerr interaction automatically and offer further promising experimental platforms for the proposed scheme. As cross-Kerr couplings are common in Josephson junction-coupled microwave cavities [68], our proposed scheme could enhance their capabilities in spite of inevitable self-Kerr coupling as well. All platforms that realize our proposed scheme can readily test the potential to stabilize the ground state for increasing bath temperature and the possibility to generate Fock states by successive shaping of the available Zeno subspaces. We aim to pursue all of these avenues in future works, as well as the correspondence of the proposed blockade, enabling only single excitations with genuine fermionic systems.

*Acknowledgments.* K.P. and A.X. would like to thank Peter Rabl and Shabir Barzanjeh for helpful discussions and acknowledge financial support from the Ministry for Education, Sport, Youth, Research and Innovation of the Government of Malta through its participation in the QuantERA ERA-NET Cofund in Quantum Technologies (project MQSens) implemented within the European Union's Horizon 2020 Programme.

*Data availability.* The data that support the findings of this article are not publicly available. The data are available from the authors upon reasonable request.


[1] B. Misra and E. C. G. Sudarshan, The Zeno's paradox in quantum theory, J. Math. Phys. **18**, 756 (1977).

[2] W. M. Itano, D. J. Heinzen, J. J. Bollinger, and D. J. Wineland, Quantum Zeno effect, Phys. Rev. A **41**, 2295 (1990).

[3] M. C. Fischer, B. Gutiérrez-Medina, and M. G. Raizen, Observation of the quantum Zeno and anti-Zeno effects in an unstable system, Phys. Rev. Lett. **87**, 040402 (2001).

[4] N. Syassen, D. M. Bauer, M. Lettner, T. Volz, D. Dietze, J. J. Garcia-Ripoll, J. I. Cirac, G. Rempe, and S. Dürr, Strong dissipation inhibits losses and induces correlations in cold molecular gases, Science **320**, 1329 (2008).

[5] B. Yan, S. A. Moses, B. Gadway, J. P. Covey, K. R. A. Hazzard, A. M. Rey, D. S. Jin, and J. Ye, Observation of dipolar spin-exchange interactions with lattice-confined polar molecules, Nature (London) **501**, 521 (2013).

[6] G. Barontini, R. Labouvie, F. Stubenrauch, A. Vogler, V. Guarrera, and H. Ott, Controlling the dynamics of an open many-body quantum system with localized dissipation, Phys. Rev. Lett. **110**, 035302 (2013).

[7] E. W. Streed, J. Mun, M. Boyd, G. K. Campbell, P. Medley, W. Ketterle, and D. E. Pritchard, Continuous and pulsed quantum Zeno effect, Phys. Rev. Lett. **97**, 260402 (2006).

[8] J. M. Raimond, P. Facchi, B. Peaudecerf, S. Pascazio, C. Sayrin, I. Dotsenko, S. Gleyzes, M. Brune, and S. Haroche, Quantum Zeno dynamics of a field in a cavity, Phys. Rev. A **86**, 032120 (2012).

[9] Y. S. Patil, S. Chakram, and M. Vengalattore, Measurement-induced localization of an ultracold lattice gas, Phys. Rev. Lett. **115**, 140402 (2015).

[10] J. M. Raimond, C. Sayrin, S. Gleyzes, I. Dotsenko, M. Brune, S. Haroche, P. Facchi, and S. Pascazio, Phase space tweezers for tailoring cavity fields by quantum Zeno dynamics, Phys. Rev. Lett. **105**, 213601 (2010).

[11] A. Signoles, A. Facon, D. Grosso, I. Dotsenko, S. Haroche, J. M. Raimond, M. Brune, and S. Gleyzes, Confined quantum Zeno dynamics of a watched atomic arrow, Nat. Phys. **10**, 715 (2014).

[12] L. Bretheau, P. Campagne-Ibarcq, E. Flurin, F. Mallet, and B. Huard, Quantum dynamics of an electromagnetic mode that cannot contain $n$ photons, Science **348**, 776 (2015).

[13] P. Facchi and S. Pascazio, Quantum Zeno dynamics: Mathematical and physical aspects, J. Phys. A: Math. Theor. **41**, 493001 (2008).

[14] Y.-P. Huang and P. Kumar, Antibunched emission of photon pairs via quantum Zeno blockade, Phys. Rev. Lett. **108**, 030502 (2012).

[15] Y.-Z. Sun, Y.-P. Huang, and P. Kumar, Photonic nonlinearities via quantum Zeno blockade, Phys. Rev. Lett. **110**, 223901 (2013).

[16] M. Aspelmeyer, T. J. Kippenberg, and F. Marquardt, Cavity optomechanics, Rev. Mod. Phys. **86**, 1391 (2014).

[17] S. Barzanjeh, A. Xuereb, S. Gröblacher, M. Paternostro, C. A. Regal, and E. M. Weig, Optomechanics for quantum technologies, Nat. Phys. **18**, 15 (2022).

[18] T. J. Kippenberg, H. Rokhsari, T. Carmon, A. Scherer, and K. J. Vahala, Analysis of radiation-pressure induced mechanical oscillation of an optical microcavity, Phys. Rev. Lett. **95**, 033901 (2005).

[19] F. Marquardt, J. G. E. Harris, and S. M. Girvin, Dynamical multistability induced by radiation pressure in high-finesse micromechanical optical cavities, Phys. Rev. Lett. **96**, 103901 (2006).

[20] J. Millen, T. Deesuwan, P. Barkere, and J. Anders, Nanoscale temperature measurements using non-equilibrium Brownian dynamics of a levitated nanosphere, Nat. Nanotechnol. **9**, 425 (2014).

[21] U. Delić, M. Reisenbauer, D. Grass, N. Kiesel, V. Vuletić, and M. Aspelmeyer, Cavity cooling of a levitated nanosphere by coherent scattering, Phys. Rev. Lett. **122**, 123602 (2019).

[22] J. D. Thompson, B. M. Zwickl, F. Marquardt, S. M. Girvin, and J. G. E. Harris, Strong dispersive coupling of a high-finesse cavity to a micromechanical membrane, Nature (London) **452**, 72 (2008).

[23] S. Gröblacher, K. Hammerer, M. R. Vanner, and M. Aspelmeyer, Observation of strong coupling between a micromechanical resonator and an optical cavity field, Nature (London) **460**, 724 (2009).

[24] J. D. Teufel, T. Donner, D. Li, J. W. Harlow, M. S. Allman, K. Cicak, A. J. Sirois, J. D. Whittaker, K. W. Lehnert, and R. W. Simmonds, Sideband cooling of micromechanical motion to the quantum ground state, Nature (London) **475**, 359 (2011).

[25] C. A. Regal, J. D. Teufel, and K. W. Lehnert, Measuring nanomechanical motion with a microwave cavity interferometer, Nat. Phys. **4**, 555 (2008).
[26] D. Bothner, S. Yanai, A. Iniguez-Rabago, M. Yuan, Y. M. Blanter, and G. A. Steele, Cavity electromechanics with parametric mechanical driving, Nat. Commun. **11**, 1589 (2020).
[27] Q. P. Unterreithmeier, E. M. Weig, and J. P. Kotthaus, Universal transduction scheme for nanomechanical systems based on dielectric forces, Nature (London) **458**, 1001 (2009).
[28] J. Bochmann, A. Vainsencher, D. D. Awschalom, and A. N. Cleland, Nanomechanical coupling between microwave and optical photons, Nat. Phys. **9**, 712 (2013).
[29] R. W. Andrews, T. P. Purdy, K. Cicak, R. W. Simmonds, C. A. Regal, and K. W. Lehnert, Bidirectional and efficient conversion between microwave and optical light, Nat. Phys. **10**, 321 (2014).
[30] S. Barzanjeh, M. Wulf, M. Peruzzo, M. Kalaee, P. B. Dieterle, O. Painter, and J. M. Fink, Mechanical on-chip microwave circulator, Nat. Commun. **8**, 953 (2017).
[31] N. R. Bernier, L. D. Tóth, A. Koottandavida, M. D. Ioannu, D. Malz, A. Nunnenkamp, A. K. Feofanov, and T. J. Kippenberg, Nonreciprocal reconfigurable microwave optomechanical circuit, Nat. Commun. **8**, 604 (2017).
[32] D. Malz, L. D. Tóth, N. R. Bernier, A. K. Feofanov, T. J. Kippenberg, and A. Nunnenkamp, Quantum-limited directional amplifiers with optomechanics, Phys. Rev. Lett. **120**, 023601 (2018).
[33] L. M. de Lépinay, E. Damskägg, C. F. Ockeloen-Korppi, and M. A. Sillanpää, Realization of directional amplification in a microwave optomechanical device, Phys. Rev. Appl. **11**, 034027 (2019).
[34] P. E. Allain, B. Guha, C. Baker, D. Parrain, A. Lemaître, G. Leo, and I. Favero, Electro-optomechanical modulation instability in a semiconductor resonator, Phys. Rev. Lett. **126**, 243901 (2021).
[35] C. F. Ockeloen-Korppi, E. Damskägg, J. M. Pirkkalainen, M. Asjad, A. A. Clerk, F. Massel, M. J. Wooley, and M. A. Sillanpää, Stabilized entanglement of massive mechanical oscillators, Nature (London) **556**, 478 (2018).
[36] R. Riedinger, A. Wallucks, I. Marinković, C. Löschnauer, M. Aspelmeyer, S. Hong, and S. Gröblacher, Remote quantum entanglement between two micromechanical oscillators, Nature (London) **556**, 473 (2018).
[37] L. Orr, S. A. Khan, N. Buchholz, S. Kotler, and A. Metelmann, High-purity entanglement of hot propagating modes using nonreciprocity, PRX Quantum **4**, 020344 (2023).
[38] K. Pelka, M. Aquilina, and A. Xuereb, Routing entanglement through quantum networks, arXiv:2402.08102.
[39] J. Chan, T. P. M. Alegre, A. H. Safavi-Naeini, J. T. Hill, A. Krause, S. Gröblacher, M. Aspelmeyer, and O. Painter, Laser cooling of a nanomechanical oscillator into its quantum ground state, Nature (London) **478**, 89 (2011).
[40] A. Schliesser, P. Del'Haye, N. Nooshi, K. J. Vahala, and T. J. Kippenberg, Radiation pressure cooling of a micromechanical oscillator using dynamical backaction, Phys. Rev. Lett. **97**, 243905 (2006).
[41] G. Heinrich, M. Ludwig, J. Qian, B. Kubala, and F. Marquardt, Collective dynamics in optomechanical arrays, Phys. Rev. Lett. **107**, 043603 (2011).
[42] M. Zhang, G. S. Wiederhecker, S. Manipatruni, A. Barnard, P. McEuen, and M. Lipson, Synchronization of micromechanical oscillators using light, Phys. Rev. Lett. **109**, 233906 (2012).
[43] M. Zhang, S. Shah, J. Cardenas, and M. Lipson, Synchronization and phase noise reduction in micromechanical oscillator arrays coupled through light, Phys. Rev. Lett. **115**, 163902 (2015).
[44] N. Lörch, S. E. Nigg, A. Nunnenkamp, R. P. Tiwari, and C. Bruder, Quantum synchronization blockade: Energy quantization hinders synchronization of identical oscillators, Phys. Rev. Lett. **118**, 243602 (2017).
[45] K. Pelka, V. Peano, and A. Xuereb, Chimera states in small optomechanical arrays, Phys. Rev. Res. **2**, 013201 (2020).
[46] D. Malz and A. Nunnenkamp, Floquet approach to bichromatically driven cavity-optomechanical systems, Phys. Rev. A **94**, 023803 (2016).
[47] H. Xu, A. A. Clerk, and J. G. E. Harris, Nonreciprocal control and cooling of phonon modes in an optomechanical system, Nature (London) **568**, 65 (2019).
[48] L. Mercadé, K. Pelka, R. Burgwal, A. Xuereb, A. Martínez, and E. Verhagen, Floquet phonon lasing in multimode optomechanical systems, Phys. Rev. Lett. **127**, 073601 (2021).
[49] K. Pelka, G. Madiot, R. Braive, and A. Xuereb, Floquet control of optomechanical bistability in multimode systems, Phys. Rev. Lett. **129**, 123603 (2022).
[50] A. Xuereb, C. Genes, and A. Dantan, Strong coupling and long-range collective interactions in optomechanical arrays, Phys. Rev. Lett. **109**, 223601 (2012).
[51] M. Schmidt, S. Kessler, V. Peano, O. Painter, and F. Marquardt, Optomechanical creation of magnetic fields for photons on a lattice, Optica **2**, 635 (2015).
[52] V. Peano, C. Brendel, M. Schmidt, and F. Marquardt, Topological phases of sound and light, Phys. Rev. X **5**, 031011 (2015).
[53] J. P. Mathew, J. del Pino, and E. Verhagen, Synthetic gauge fields for phonon transport in a nano-optomechanical system, Nat. Nanotechnol. **15**, 198 (2020).
[54] D. J. Wilson, C. A. Regal, S. B. Papp, and H. J. Kimble, Cavity optomechanics with stoichiometric SiN films, Phys. Rev. Lett. **103**, 207204 (2009).
[55] J. C. Sankey, C. Yang, B. M. Zwickl, A. M. Jayich, and J. G. E. Harris, Strong and tunable nonlinear optomechanical coupling in a low-loss system, Nat. Phys. **6**, 707 (2010).
[56] C. Reinhardt, T. Müller, A. Bourassa, and J. C. Sankey, Ultralow-noise SiN trampoline resonators for sensing and optomechanics, Phys. Rev. X **6**, 021001 (2016).
[57] T. P. Purdy, D. W. C. Brooks, T. Botter, N. Brahms, Z.-Y. Ma, and D. M. Stamper-Kurn, Tunable cavity optomechanics with ultracold atoms, Phys. Rev. Lett. **105**, 133602 (2010).
[58] T. T. Heikkilä, F. Massel, J. Tuorila, R. Khan, and M. A. Sillanpää, Enhancing optomechanical coupling via the Josephson effect, Phys. Rev. Lett. **112**, 203603 (2014).
[59] H. Solki, A. Motazedifard, and M. H. Naderi, Improving photon blockade, entanglement, and mechanical-cat-state generation in a generalized cross-Kerr optomechanical circuit, Phys. Rev. A **108**, 063505 (2023).
[60] P. Rabl, Photon blockade effect in optomechanical systems, Phys. Rev. Lett. **107**, 063601 (2011).
[61] Y. Chu, P. Kharel, T. Yoon, L. Frunzio, P. T. Rakich, and R. J. Schoelkopf, Creation and control of multi-phonon Fock states in a bulk acoustic-wave resonator, Nature (London) **563**, 666 (2018).
[62] Q. R. Rahman, I. Kladarić, M.-E. Kern, L. Lachman, Y. Chu, R. Filip, and M. Fadel, Genuine quantum non-Gaussianity and

metrological sensitivity of Fock states prepared in a mechanical resonator, Phys. Rev. Lett. **134**, 180801 (2025).

[63] K. Stannigel, P. Komar, S. J. M. Habraken, S. D. Bennett, M. D. Lukin, P. Zoller, and P. Rabl, Optomechanical quantum information processing with photons and phonons, Phys. Rev. Lett. **109**, 013603 (2012).

[64] P. Facchi, Quantum Zeno effect, adiabacity and dynamical superselection rules, Fundam. Aspects Quantum Phys. **17**, 197 (2011).

[65] See Supplemental Material at http://link.aps.org/supplemental/10.1103/vhnq-79bj for the determination of distinct Zeno subspaces in bosonic systems, the formation of Zeno subspaces in nondiagonal Hamiltonians, analysis of potential perturbing nonlinearities and their negligible impact, and a description of a multitone blockade to prepare a one phonon state with a high fidelity.

[66] C. Gardiner and P. Zoller, The master equation, in *Quantum Noise*, 2nd ed., edited by H. Haken (Springer, New York, 2000), pp. 161–168.

[67] J.-M. Pirkkalainen, S. U. Cho, F. Massel, J. Tuorila, T. T. Heikkilä, P. J Hakonen, and M. A. Sillanpää, Cavity optomechanics mediated by a quantum two-level system, Nat. Commun. **6**, 6981 (2015).

[68] E. T. Holland, B. Vlastakis, R. W. Heeres, M. J. Reagor, U. Vool, Z. Leghtas, L. Frunzio, G. Kirchmair, M. H. Devoret, M. Mirrahimi, and R. J. Schoelkopf, Single-photon-resolved cross-Kerr interaction for autonomous stabilization of photon-number states, Phys. Rev. Lett. **115**, 180501 (2015).